Expression of the P2X₂ Receptor Subunit of the ATP-Gated Ion Channel in the Cochlea: Implications for Sound Transduction and Auditory Neurotransmission

Gary D. Housley,[1] Refik Kanjhan,[1] Nicholas P. Raybould,[1] Denise Greenwood,[1] Salam G. Salih,[1] Leif Järlebark,[1] Lucille D. Burton,[1] Vera C. M. Setz,[1] Mark B. Cannell,[1] Christian Soeller,[1] David L. Christie,[2] Shin-ichi Usami,[3] Atsushi Matsubara,[3] Haruhide Yoshie,[3] Allen F. Ryan,[4] and Peter R. Thorne[1]

[1]Department of Physiology, Faculty of Medicine and Health Science and [2]School of Biological Sciences, University of Auckland, Private Bag 92019, Auckland, New Zealand, [3]Department of Otorhinolaryngology, Hirosaki University School of Medicine, Hirosaki 036-8562, Japan, and [4]Departments of Surgery and Neuroscience, University of California San Diego, La Jolla, California 92093

Extracellular ATP has multimodal actions in the cochlea affecting hearing sensitivity. ATP-gated ion channels involved in this process were characterized in the guinea pig cochlea. Voltage-clamped hair cells exhibited a P2 receptor pharmacology compatible with the assembly of ATP-gated ion channels from P2X₂ receptor subunits. Reverse transcription-PCR experiments confirmed expression of the P2X₂₋₁ receptor subunit mRNA isoform in the sensory epithelium (organ of Corti); a splice variant that confers desensitization, P2X₂₋₂, was the predominant subunit isoform expressed by primary auditory neurons. Expression of the ATP-gated ion channel protein was localized using a P2X₂ receptor subunit-specific antiserum. The highest density of P2X₂ subunit-like immunoreactivity in the cochlea occurred on the hair cell stereocilia, which faces the endolymph. Tissues lining this compartment exhibited significant P2X₂ receptor subunit expression, with the exception of the stria vascularis. Expression of ATP-gated ion channels at these sites provides a pathway for the observed ATP-induced reduction in endocochlear potential and likely serves a protective role, decoupling the "cochlear amplifier" in response to stressors, such as noise and ischemia. Within the perilymphatic compartment, immunolabeling on Deiters' cells is compatible with purinergic modulation of cochlear micromechanics. P2X₂ receptor subunit expression was also detected in spiral ganglion primary afferent neurons, and immunoelectron microscopy localized these subunits to postsynaptic junctions at both inner and outer hair cells. The former supports a cotransmitter role for ATP in a subset of type I spiral ganglion neurons, and latter represents the first characterization of a receptor for a fast neurotransmitter associated with the type II spiral ganglion neurons.

Key words: P2X₂ receptor; organ of Corti; cochlea; immunocytochemistry; hair cell stereocilia; spiral ganglion; guinea pig; hearing; ATP; auditory neurotransmission; inner hair cells; outer hair cells; sound transduction

The majority of sensory systems exhibit ATP signaling (Burnstock, 1996; Thorne and Housley, 1996; Cook et al., 1997; Greenwood et al., 1997; Housley, 1999), with the cochlea in particular appearing to function under a multimodal influence of extracellular ATP (for review, see Thorne and Housley, 1996; Housley, 1998, 1999).

Recent studies indicate the storage (White et al., 1995) and Ca^{2+}-dependent release (Wangemann, 1996) of ATP from cochlear tissues. In addition, electrophysiological and imaging evidence indicates that ATP-gated ion channels, assembled from P2X receptor subunits, are a principal element of purinoceptor signal transduction mechanisms in the cochlea. ATP-activated conductances have been characterized from sensory and support-

ing cells of the guinea pig organ of Corti (Housley et al., 1992, 1993, 1998a; Mockett et al., 1994; Sugasawa et al., 1996; Thorne and Housley, 1996; King et al., 1998). In the rat, the P2X₂ receptor subunit likely contributes to the assembly of these ATP-gated ion channels on the basis of experiments using the reverse transcription (RT)-PCR (Glowatzki et al., 1995; Housley et al., 1995; Brändle et al., 1997) and *in situ* hybridization (Housley and Ryan, 1997; Housley et al., 1998b).
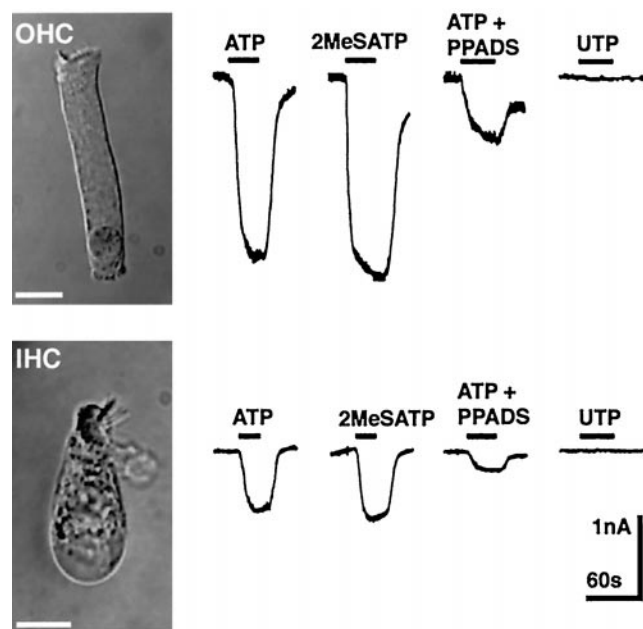
In vivo experiments provide substantive evidence for extracellular ATP-mediated alterations in cochlear function. There is a dose-dependent reduction in the endocochlear potential (a +80 mV biopotential contributing to the driving force for sound transduction) when ATP is introduced into scala media of the guinea pig (Muñoz et al., 1995a; Kirk and Yates, 1998). Perilymphatic perfusions of ATP and related agonists decrease cochlear sensitivity (increased threshold of the auditory nerve compound action potential), whereas action of P2X receptor-selective antagonists produce an inhibition of the distortion product otoacoustic emission attributable to endogenous ATP action on cochlear micromechanics (Bobbin and Thompson, 1978; Kujawa et al., 1994; Chen et al., 1998). Purinergic signaling in both the endolymphatic and perilymphatic compartments of the cochlea are

Figure 1. Whole-cell voltage-clamp analysis of P2X receptor pharmacology of cochlear hair cells. ATP and 2MeSATP (10 μM) gave sustained inward current responses. PPADS (10 μM) blocked this effect. The cells were unresponsive to UTP (100 μM). Holding potential, −60 mV. Scale bars, 12 μm.

terminated by ectonucleotidase activity (Vlajkovic et al., 1998a,b).

Recent localization of P2X$_2$ receptor mRNA expression in a subpopulation of rat cochlear spiral ganglion neurons (auditory primary afferent neurons) indicates that extracellular ATP may be directly involved in auditory neurotransmission (Salih et al., 1998).

Here, we report the expression sites of the P2X$_2$ receptor subunit of the ATP-gated ion channel in the guinea pig cochlea. These data provide a detailed insight into multimodal purinergic signaling in the cochlea and identify a number of processes that impact on the physiology of hearing, including the localization of P2X$_2$ receptors on the hair cell stereocilia and at hair cell–primary auditory neuron synapses.

MATERIALS AND METHODS

Experiments were performed on cochlear tissues obtained from adult pigmented and albino guinea pigs (both sexes, 250–800 gm) overdosed by pentobarbital following University of Auckland Animal Ethics Committee approved guidelines.

Cochlear hair cell voltage-clamp experiments. The organ of Corti was microdissected from the cochlea and briefly incubated in phosphate-buffered trypsin solution (0.5 mg/ml, 10 min; Sigma, St. Louis, MO). After trituration to aid dispersal, the hair cells were placed in a 100 μl laminar flow bath on the stage of an inverted microscope (Diaphot TMD; Nikon, Tokyo, Japan). The composition of the extracellular solution was (in mM): 152 NaCl, 4 KCl, 1.5 CaCl$_2$, 1 MgCl$_2$, 8 Na$_2$HPO$_4$, 2 NaH$_2$PO$_4$, and 3 D-glucose; osmolality of 310 mOsm, pH 7.25, adjusted with 1 M NaOH. Hair cells were voltage-clamped at room temperature using an

Axopatch 200 patch-clamp amplifier (Axon Instruments, Foster City, CA) as described previously (Raybould and Housley, 1997). The internal solution was (in mM): 150 KCl, 0.01 CaCl$_2$, 2 MgCl$_2$, 8 Na$_2$HPO$_4$, 1 NaH$_2$PO$_4$, 0.5 EGTA and 3 D-glucose; osmolality of 305 mOsm, pH 7.25, adjusted with 1 M KOH. The electrodes were pulled to an input resistance of 2–5 MΩ from borosilicate glass (GC120, TF-10; Clark Electromedical Instruments, Pangbourne, UK). Junction offset potentials were cancelled before tight-seal formation, and after establishment of whole-cell recording, series resistance was 95% compensated on-line. ATP, related agonists (10–100 μM), the P2X receptor antagonist pyridoxal-phosphate-6-azophenyl-2′,4′-disulphonic acid (PPADS) (10 μM; Research Biochemicals, Natick, MA, and the P2X$_2$R96ab antiserum (1:20–1:100 dilution) were applied by rapid bath substitution (200 μl/min). Electrophysiological data were acquired using an analog-to-digital board (Tecmar TL-1, Labmaster; Scientific Solutions, Mentor, OH) and pClamp 5.0 software (Axon Instruments) and continuously recorded on digital audio tape (RD 101T; Teac, Tokyo, Japan). Hair cell images were recorded on videotape for size analysis.

Analysis of P2X$_2$ receptor mRNA expression. The cDNA templates for RT-PCR were obtained by reverse transcribing mRNA isolated from microdissected organ of Corti (10 cochleas) or spiral ganglion (two cochleas) as described previously (King et al., 1998; Salih et al., 1998) using a guanidinium thiocyanate-based extraction procedure (QuickPrep Micro mRNA purification kit; Amersham Pharmacia Biotech, Piscataway, NJ). Eluted poly(A$^+$)-selected mRNA (3.5 μl of the 200 μl available) provided template for reverse transcription [20 μl RT reaction: 50 units Moloney murine leukemia virus (MMLV) reverse transcriptase (Perkin-Elmer, Emeryville, CA), oligo(dT)$_{12–18}$ primer (25 pg), 2.5 mM dNTPs (Life Technologies, Gaithersburg, MD), and 10 μM RNase inhibitor (Boehringer Mannheim, Mannheim, Germany) at 42°C for 45 min]. PCR reactions used 2 μl of the RT reaction product for cDNA template. Control PCR experiments included equivalent quantities of mRNA, omitting the reverse transcriptase. PCR primers (20-mer sense and 21-mer antisense oligonucleotides) corresponded to 3′ and 5′ positions 756 and 1558, respectively, of the rat P2X$_2$ receptor cDNA sequence (GenBank accession number U14414) (Brake et al., 1994). The primers were used at 2.5 μM concentration in a 50 μl PCR reaction containing 2.5 U Ampli*Taq* DNA polymerase (Perkin-Elmer), 1.25 mM MgCl$_2$, 200 μM dNTP, using a thermal cycle profile of 94°C for 1 min, 60°C for 1 min, and 72°C for 2 min, for 30 cycles. P2X$_{2-1}$ receptor cDNAs were ligated into pCRII plasmid (Invitrogen, San Diego, CA) and transformed into OneShot competent cells (Invitrogen) for isolation and sequencing (ABI 373A sequencer; Applied Biosystems, Foster City, CA).

Immunolocalization of P2X$_2$ receptor protein expression. Tissue was fixed by transcardial perfusion with 4% formaldehyde (BDH Laboratory Supplies, Poole, UK) and 0.5% glutaraldehyde (EM-grade; Merck, Darmstadt, Germany) in 0.1 M PBS. The cochleas were then post-fixed overnight after injection of this solution into the scalae. Whole-mount preparations were prepared by dissecting individual turns of the cochlea, removal of the tectorial membrane, and resection of the lateral wall. The cochlear turns were then preincubated in 1% bovine serum albumin (Sigma) in PBS or 1.5% normal goat serum (Vector Laboratories, Burlingame, CA) for 1 hr before incubation in the P2X$_2$R96ab antiserum (1:1000–1:4000) overnight at 4°C. The antiserum was raised in rabbit against an 18 amino acid sequence (96–113) of the extracellular domain of the rat P2X$_2$ receptor subunit (Brake et al., 1994) and has cross-reactivity with the guinea pig P2X$_2$ receptor homolog (Kanjhan et al., 1996) but not with other P2X receptor subtypes (Kanjhan et al., 1999). The P2X$_2$R96ab antiserum was stored in 50 μg/ml keyhole limpet hemocyanin (Sigma). The tissue was then washed in PBS and incubated in biotinylated goat anti-rabbit IgG (1:400–1:800; Sigma) for 4–6 hr. The tissue was again washed and then incubated overnight at 4°C in ExtrAvidin–peroxidase (1:1000–1:2000; Sigma). After final washing in PBS, the tissue was washed in Tris-HCl buffer (0.05 M, pH 7.6) and then reacted with chromogen solution containing: 3,3′-diaminobenzidine (0.5 mg/ml; Sigma), H$_2$O$_2$ (0.001–0.01%), and nickel ammonium sulfate (6

Table 1. P2 receptor agonist and antagonist profiles and biophysical properties

	ATP (pA)	2MeSATP (pA)	(*n*)	ATP (pA)	ATP $\pm$ PPADS (pA)	(*n*)	Length (μm)	C_m (pF)	V_z (mV)	(*n*)
OHC	−1673 $\pm$ 275	−1877 $\pm$ 315	16	−1849 $\pm$ 565	−602 $\pm$ 200	5	41.2–74.6	12.6–43.6	−66.3 $\pm$ 1.4	17
IHC	−809 $\pm$ 79	−1092 $\pm$ 128	10	−683 $\pm$ 98	−231 $\pm$ 26	5	25.2–32.4	8.8–16.5	−49.5 $\pm$ 1.8	10

Mean $\pm$ SEM; C_m, membrane capacitance; V_z, zero current potential. ATP, 2 MeSATP, PPADS, all 10 μM.

organ of Corti
P2X$_{2-1}$R

spiral ganglion
P2X$_{2-2}$R
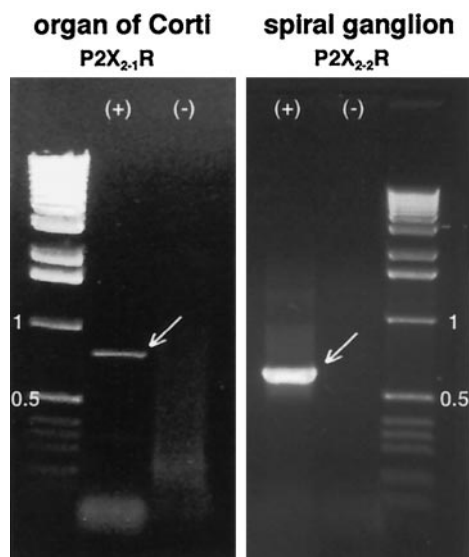
Figure 2. Molecular characterization of P2X$_2$ receptor expression in sensory and neural epithelium. Agarose gels showing an 803 bp P2X$_{2-1}$ receptor isoform RT-PCR product derived from organ of Corti mRNA template and a 596 bp RT-PCR product (P2X$_{2-2}$ receptor isoform) derived from spiral ganglion mRNA. +, Indicates reverse-transcribed mRNA; −, indicates omission of the MMLV reverse transcriptase.

mg/ml). Cochlear tissue was cryosectioned at 35 μm with or without 2 weeks of decalcification in 10% EDTA in the fixative solution, pH 7.4, and cryoprotection (10–30% sucrose in 0.1 M PBS). Floating cochlear sections were processed for immunoperoxidase histochemistry as described above. P2X$_2$ receptor immunoreactivity was localized on cochlear outer hair cells (OHC) that had been isolated as described for electrophysiological analysis. The cells were serially incubated for 10–20 min in external solutions containing: P2X$_2$R96ab antiserum (1:20–1:100), biotinylated goat anti-rabbit IgG (1:20), and then a suspension (1:10) of avidin-conjugated 0.2 μm latex FluoSpheres (Molecular Probes, Eugene, OR), separated by washes. The cells were imaged in light-field using Nomarski differential interference contrast optics and epifluorescence-mode using a fluorescein isothiocyanate (FITC) filter set (XF22; Omega Optical Inc., Brattleboro, VT). In control experiments, OHC were incubated without primary antiserum.

Confocal microscopy was used to examine both whole-mount and cryosectioned cochlear tissue. Whole-mount tissue (three experiments) was examined using a Leica confocal microscope (TCSAD; Leica Lasertechnik GmbH, Heidelberg, Germany) using 568 nm light from an argon–krypton laser as described previously (King et al., 1998). Immunofluorescence of nondecalcified cryosectioned cochlear tissue (five experiments) was examined using a two-photon microscope system (Soeller and Cannell, 1996) in which light at 850 nm and 100 fsec pulse duration was used to excite the Alexa 488 fluorophore (1:400; Molecular Probes) after incubation in primary antiserum (1:400). The whole-mount tissue was incubated overnight in primary antiserum (1:1000) and, after washing in PBS, was incubated in Cy3-conjugated secondary fluorescence antibody (1:500; Amersham Life Science Ltd, Buckinghamshire, UK) for 2–4 hr at room temperature for confocal imaging or in Alexa 488 secondary antibody for two-photon fluorescence imaging. The tissue was then washed and mounted in wells on slides using Dako fluorescent mounting medium (Dako, Carpinteria, CA). Image analysis included
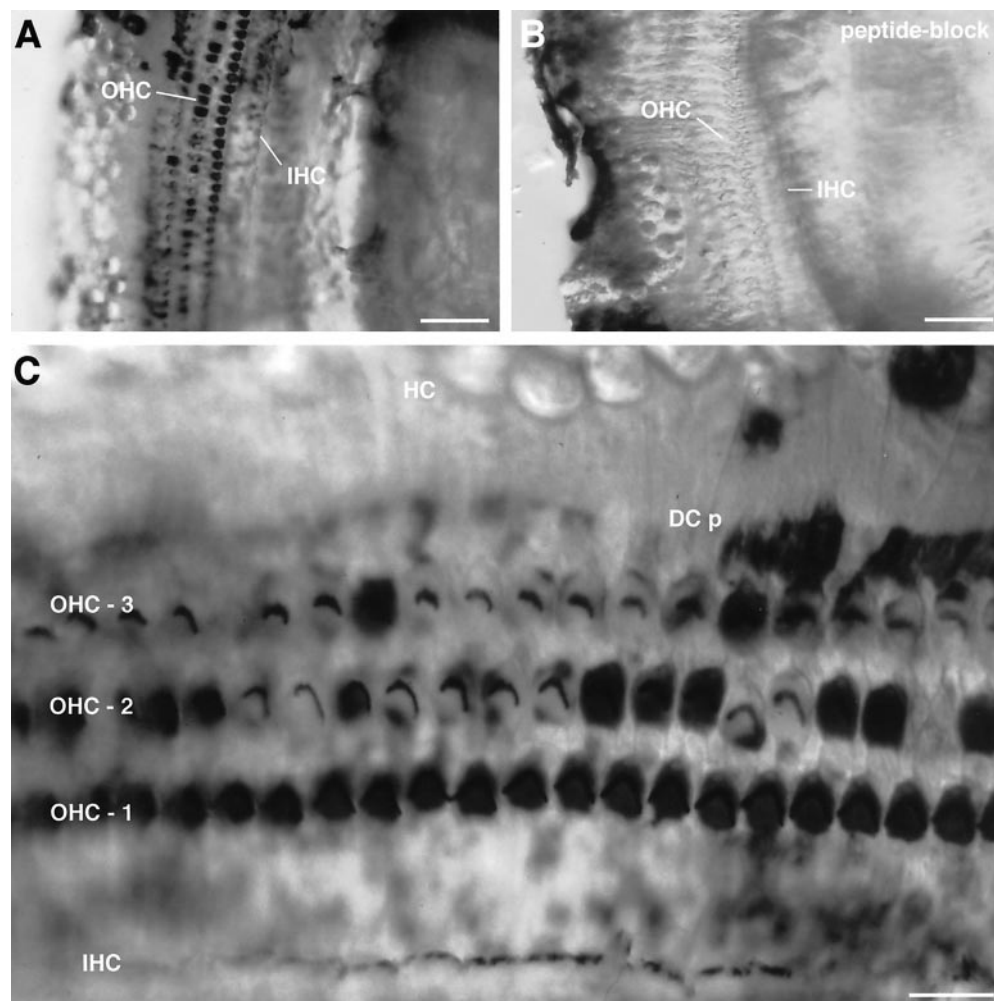
Figure 3. Identification of P2X$_2$ receptor protein expression in the organ of Corti. *A,* Whole-mount surface preparation of turn three of the guinea pig organ of Corti using immunoperoxidase histochemistry. Note the intense P2X$_2$ receptor-immunopositive labeling of the three rows of OHC and the single row of IHC. *B,* Control for specificity of the P2X$_2$R96ab antiserum was demonstrated by block of the immunolabeling by preadsorption with the target 18 amino acid peptide (10 μg/ml). *A* and *B* were adjacent regions of organ of Corti tissue (P2X$_2$R96ab antiserum, 1:2000). *C,* Detail of third turn organ of Corti region showing that the most intense P2X$_2$ receptor immunolabeling occurred on the stereocilia. Note the lack of immunolabeling on the endolymphatic surfaces of the Deiters' cell processes (*DCp*), except for *row 3* (P2X$_2$R96ab antiserum, 1:2000). Scale bars: *A, B,* 50 μm; *C,* 15 μm.

Figure 4. Localization of P2X$_2$ receptor subunits on hair cell stereocilia. *A*, Detail of P2X$_2$ receptor immunolabeling of *row 2* OHC stereocilia from the third turn of the cochlea (*arrows*) (P2X$_2$R96ab antiserum, 1:4000). *B*, *C*, Light-field and immunofluorescence images, respectively, of an isolated guinea pig OHC showing binding of avidin-linked FITC microspheres to the stereocilia (*arrows*) (P2X$_2$R96ab antiserum, 1:20). Labeling is also apparent on processes attached to the base of the OHC, which likely correspond to synaptic terminals (*). Scale bars, 5 μm.
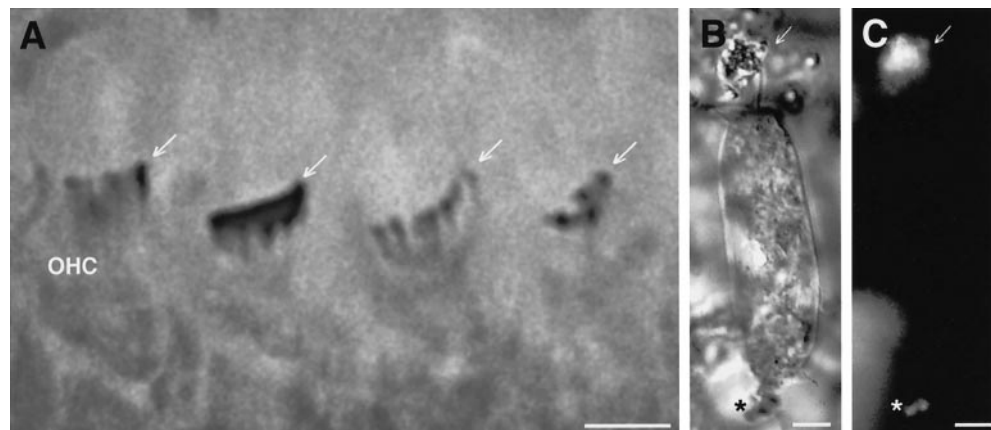
three-dimensional reconstruction of voxels obtained from serial confocal images using VoxelView software (Vital Images Inc., Minneapolis, MN) and isosurface rendering of data sets using Iris Explorer software (Silicon Graphics, Mountain View, CA).

For immunoelectron microscopy, the cochlear tissues were fixed (Usami et al., 1992) in 4% formaldehyde and 0.5% glutaraldehyde, cryoprotected, quick frozen, freeze-substituted, and low-temperature embedded in a methacrylate resin (Lowicryl HM 20; Chemische Werke Lowi, Waldkraiburg, Germany) according to Matsubara et al. (1996). Postembedding immunogold staining was performed using ultrathin sections briefly (2–3 sec) immersed in a saturated solution of NaOH in absolute ethanol, rinsed well with double-distilled water, and incubated in the following solutions (at room temperature): (1) 0.1% sodium borohydride and 50 mM glycine in Tris-buffered saline containing 0.1% Triton X-100 (TBST) (10 min); (2) 2% human serum albumin (HSA) in TBST (10 min); (3) primary antibodies against P2X$_2$ (1:500) in TBST containing 2% HSA (4°C, overnight); (4) 2% HSA in TBST (10 min); and (5) secondary goat anti-rabbit IgG 15 nm gold-coupled antiserum (AuroProbe; Amersham Life Science Limited) diluted 1:20 in TBST containing 2% HSA and polyethyleneglycol (5 mg/ml, 2 hr). The sections were rinsed well between steps 3 and 5. The sections were counterstained by uranyl acetate and lead citrate and examined in a JEOL (Akishima, Japan) 100CX electron microscope.

RESULTS

Characterization of hair cell responses to P2 receptor agonists and antagonists

Whole-cell voltage-clamp analysis was performed to functionally characterize the ATP-gated ion channels in the hair cells of the guinea pig cochlea (Fig. 1). The ATP-activated conductances of both inner hair cells (IHC) and OHC exhibited pharmacological profiles compatible with that of the heterologously expressed P2X$_2$ receptor subtype (Brake et al., 1994; Buell et al., 1996). The ATP analog 2-methylthio-ATP (2MeSATP) (10 μM) elicited significantly greater sustained inward currents (Student's paired *t* test; OHC, $p < 0.05$; IHC, $p < 0.01$) than ATP (10 μM) at a holding potential of −60 mV (Table 1). PPADS (10 μM) blocked the ATP-gated inward current by $57.7 \pm 6.7\%$ in OHC ($p < 0.01$) and by $64.9 \pm 3.1\%$ in IHC ($p < 0.01$) (Table 1). UTP (100 μM) did not generate a detectable inward current in either cell type (OHC, $n = 5$; IHC, $n = 4$). The lack of a rapidly desensitizing response to ATP, efficacy of 2MeSATP, and the block of the ATP-activated inward current by PPADS, which is ineffective for P2X$_4$ or P2X$_6$ receptor subtypes (Buell et al., 1996; Collo et al., 1996; North, 1996), are all consistent with a P2X$_2$ receptor subtype classification.

Characterization of P2X$_2$ receptor mRNA expression

RT-PCR experiments confirmed the expression of the P2X$_2$ receptor subunit mRNA in the guinea pig organ of Corti and spiral

ganglion and demonstrated a differential expression of splice variants in the sensory epithelium versus neuronal tissue (Fig. 2). An 803 bp P2X$_2$ receptor PCR product was detected using reverse transcribed mRNA from the organ of Corti as template, whereas the spiral ganglion cDNA template yielded a smaller amplicon (596 bp). The organ of Corti P2X$_2$ receptor cDNA sequence was 99% identical with the corresponding rat P2X$_{2-1}$ receptor cDNA homolog cloned from PC12 cells (Brake et al., 1994) and was identical to a 500 bp cDNA previously isolated from guinea pig Reissner's membrane (GenBank accession number AF062035) (King et al., 1998). The additional 303 bp of 3′ sequence contained a single nucleotide substitution (A–G), equivalent to position 846 of the rat P2X$_2$ receptor isoform cDNA sequence (GenBank accession number U14414) (Brake et al., 1994), conserving the coding of Lys[270]. The smaller PCR product obtained from the spiral ganglion neuron cDNA template corresponded to the alternatively spliced isoform P2X$_{2-2}$, previously identified from rat cochlea and brain and reported to generate a desensitizing inward current when expressed as a homomultimer (Brändle et al., 1997).

Immunolocalization of the P2X$_2$ receptor subunit of ATP-gated ion channels

The P2X$_2$R96ab antiserum used to localize ATP-gated ion channels in cochlear tissue targets the putative extracellular domain of the P2X$_2$ subunit, away from ligand binding or pore-lining sites, and does not discriminate between P2X$_2$ receptor isoforms arising from alternative splicing of the 5′ coding region. The antiserum (1:20) did not affect ATP-activated inward currents in OHC voltage-clamped at −60 mV (paired Student's *t* test; $p > 0.05$; $n = 4$). Mean ($\pm$ SEM) response to 100 μM ATP was $−1005 \pm 347$ pA compared with an average of $−937 \pm 369$ pA after 140–280 of superfusion with the antiserum. Onset and washout kinetics of the ATP responses were also unaffected by incubation with the antiserum. The cell lengths and biophysical properties of the OHC fell within the normal range for these cells described in Table 1.

The strongest P2X$_2$ receptor immunolabeling was found on the apical aspect of the stereocilia of the IHC and OHC, within the endolymphatic compartment of the cochlea (Figs. 3–6, 10). In whole-mount preparations (10 experiments), there was no discernible difference between the density of immunoperoxidase reaction product on stereocilia of hair cells from different turns of the organ of Corti or with respect to different rows of OHC (Figs. 3*C*, 5*A,B*). However, variability in labeling of the cuticular plate regions of some IHC and OHC was apparent (Fig. 3*C*, 5*A*, 10*A*).
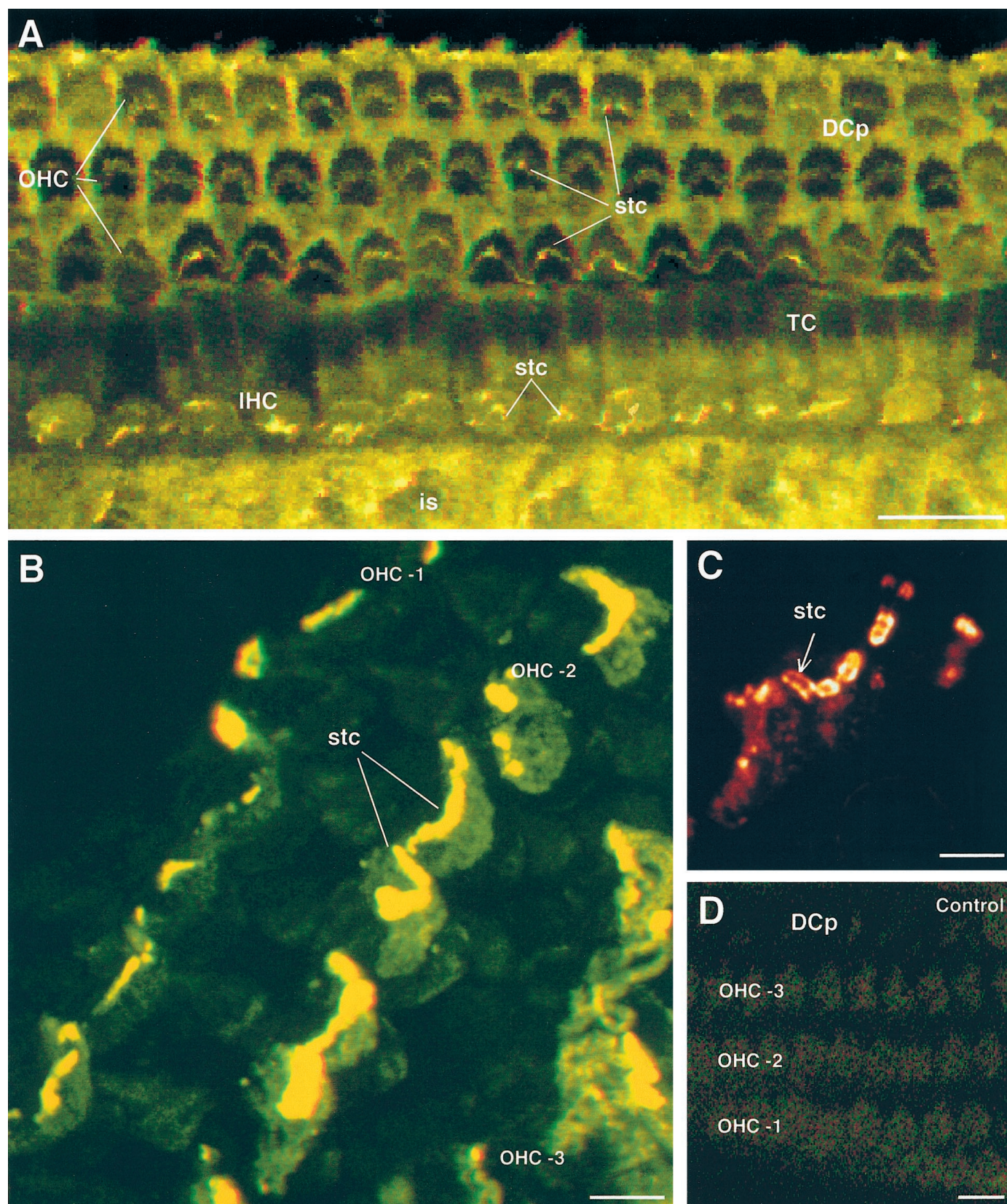
Figure 5. P2X₂ receptor immunofluorescence labeling of the organ of Corti imaged by stereo-confocal reconstruction. *A*, *Red–green* stereo-image derived from 25 confocal sections spanning 15 μm from the tips of the hair cell stereocilia (*stc*) in turn one organ of Corti. Note that the apical-most region of the OHC stereocilia shows the greatest P2X₂ receptor immunofluorescence, with little labeling on the cuticular plates. Labeling of the Deiters' cell processes (*DCp*) clearly lies below the hair cell cuticular plate level, within the perilymphatic space. The lack of labeling of the reticular lamina aspect of the pillar cells permits a view into the tunnel of Corti (*TC*). The endolymphatic surface of the IHC, particularly (*Figure legend continues*)
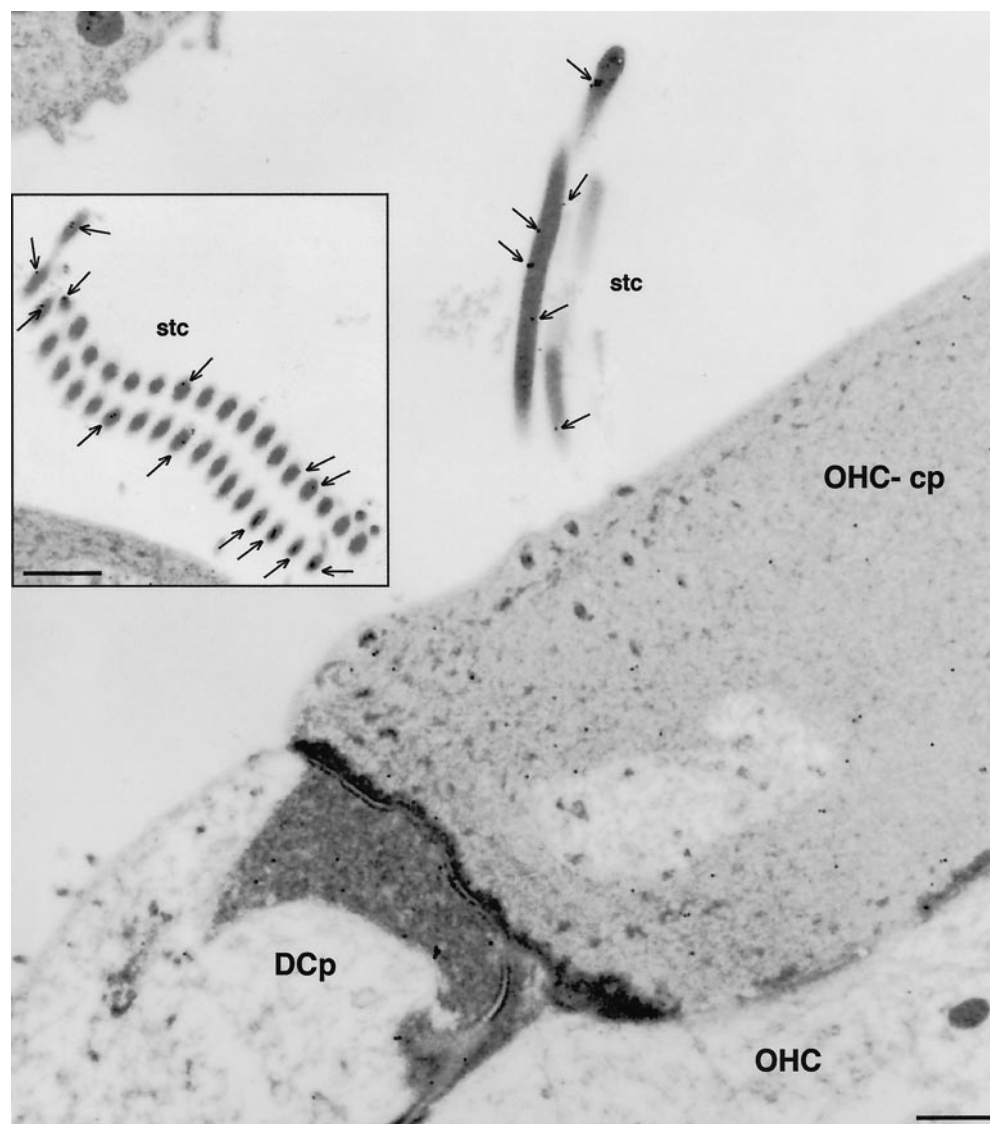
Figure 6. Electron microscopic immunolocalization of the P2X$_2$ receptor protein to the stereocilia of the guinea pig OHC. Immunogold labeling (15 nm particles) were detected at greatest density in association with the membrane of the OHC stereocilia (*stc*; *arrows*). Immunolabeling on the endolymphatic aspect of the cuticular plate (*OHC-cp*) was minimal, as was the labeling on the adjacent Deiters' cell process (*DCp*). *Inset* shows P2X$_2$ receptor immunolabeling in a cross section through the stereocilia. Scale bars: 500 nm; *inset*, 1 μm.

Damage to the tips of some stereocilia during preparation of surface mounts probably contributed to some of the variability in the immunolabeling of stereocilia of adjacent hair cells (Fig. 5B). Labeling of the endolymphatic surface of supporting cells, such as the Hensen's cells and third row Deiters' cell processes was also observed; the Deiters' cell processes medial to the outermost row of OHC were not labeled on the endolymphatic surface. This was most apparent from immunoperoxidase surface-mount preparations (Fig. 3C) and stereo reconstructions of confocal immunofluorescence of the apical aspect of the organ of Corti (Fig. 5A).

The immunolabeling was absent if the primary antiserum was omitted (Fig. 5D) and was blocked by preadsorption of the primary antiserum (1:2000) with the target peptide (10 μg/ml) (Fig. 3B). Brief peroxidase development times (<2 min) using an antibody titer of 1:4000 resulted in P2X$_2$ receptor-immunopositive labeling confined to the tip regions of the hair cell stereocilia (Fig. 4A), indicating that this was the site with the highest density of P2X$_2$ receptor subunit expression.

Confirmation that the hair cells had P2X$_2$ receptor protein confined to the endolymphatic surface was obtained in vital isolated OHC using avidin-conjugated FITC-labeled fluorescence microspheres (Fig. 4B,C) by analysis of immunolabeling obtained from cross sections of the organ of Corti (Fig. 7A,C) and, in three experiments, by reconstruction of image stacks obtained using confocal immunofluorescence (Fig. 10). The inner sulcus cells and interdental cells of the spiral limbus showed moderate levels of P2X$_2$ receptor immunolabeling, as did the epithelial cells lateral to the reticular lamina, including Claudius'

←

the stereocilia, show immunolabeling. Inner sulcus cells, *is*. *B*, Stereo reconstruction of immunolabeling on the OHC stereocilia (*rows 1–3*) showing that the brightest immunofluorescence occurs at the tip region. *C*, Confocal optical section (0.5 μm) of P2X$_2$ receptor immunofluorescence at high magnification through the tip region of the stereocilia of an OHC. Note that the P2X$_2$ receptor immunolabeling is on the outside of individual stereocilia (*stc*, *arrow*). Both *B* and *C* are from turn three of the organ of Corti. *D* is from the turn one to two region. *D*, Control confocal immunofluorescence image of organ of Corti tissue (omission of P2X$_2$R96ab antiserum; secondary antibody, Cy3-conjugated goat anti-rabbit IgG, 1:500). Scale bars: *A*, 10 μm; *B*, *C*, 4 μm; *D*, 10 μm.
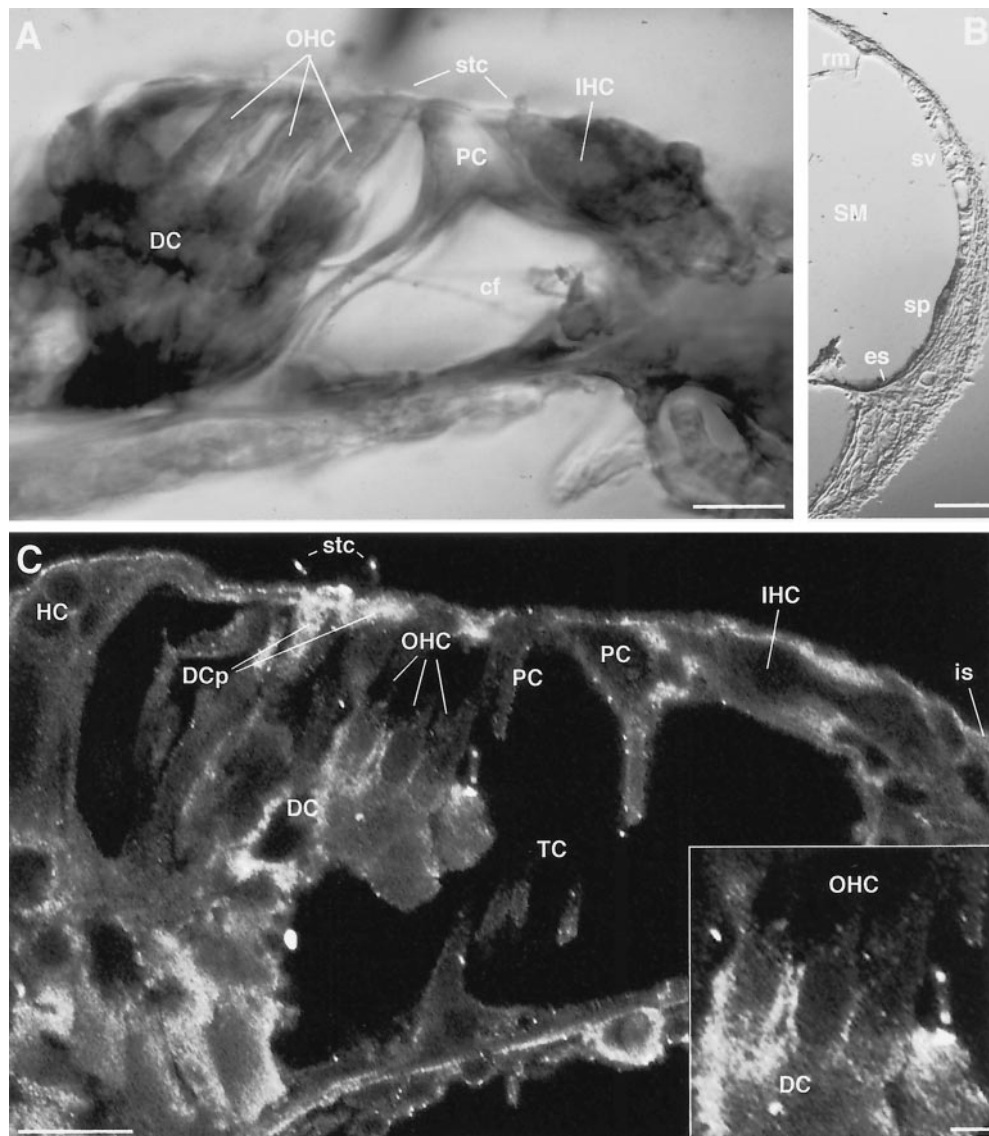
Figure 7. P2X$_2$ receptor immunolabeling of radial sections of the cochlea. *A*, P2X$_2$ receptor immunoperoxidase labeling of a radial section of organ of Corti (30 μm cryosection; P2X$_2$R96ab antiserum, 1:2000). OHC are unlabeled apart from the stereocilia (*stc*). Deiters' cells (*DC*) and their processes show immunolabeling, as does the synaptic region adjacent to the IHC. Pillar cell, *PC*; crossing fibers, *cf. B*, Immunoperoxidase labeling of the spiral ligament. Note the P2X$_2$ receptor expression in the external sulcus cell (*es*), root cell region leading to the spiral prominence (*sp*), whereas the stria vascularis (*sv*) does not express these ATP-gated ion channel subunits (Reissner's membrane, *rm*; scala media, *SM*). *C*, Two-photon immunofluorescence optical section (0.9 μm) showing strong P2X$_2$ receptor immunolabeling at a number of sites in a radial section through the organ of Corti. Detail of the labeling in the Deiters' cell (*DC*) cup region is shown in the inset [P2X$_2$R96ab antiserum, 1:400; secondary antiserum (Alexa 488-conjugated goat antirabbit IgG), 1:400; 35 μm cryosection]. Deiters' cell process, *DCp*; Hensen's cell, *HC*; inner sulcus cell, *is*; tunnel of Corti, *TC*. Scale bars: *A,* 20 μm; *B*, 50 μm; *C*, 20 μm; *inset*, 5 μm.

cells and external sulcus cells (Figs. 5*A*, 7*B*, 10*A*); immunolabeling terminated laterally at the spiral prominence, and the stria vascularis exhibited negligible label (Fig. 7*B*). P2X$_2$ receptor immunolabeling of the epithelial cells of Reissner's membrane (Fig. 7*B*) using this antiserum has been reported previously (King et al., 1998) and was relatively weak compared with the other P2X$_2$ receptor-immunopositive sites lining scala media.

Immunoelectron microscopy confirmed that the greatest density of P2X$_2$ receptor subunit expression was on the stereocilia of the OHC (Fig. 6) in which numerous 15 nm gold particles were associated with the plasma membrane. In contrast, few gold particles were evident on the endolymphatic surface of the cuticular plates of the hair cells, or within the bulk of the hair cell or the Deiters' cell cytoplasm.

Within the perilymphatic compartment, the Deiters' cells showed substantial immunostaining, including the Deiters' cell processes, which extend to the reticular lamina to support the apical aspect of the OHC, and the cup region, which encompasses the basal, synaptic pole of the OHC (Figs. 5*A*, 7*A,C inset*, 8*A, B*, 10*B–D*). Pillar cells also exhibited P2X$_2$ receptor immunolabeling in the perilymphatic compartment, although this was very

weak, except for the foot process and the border with the inner phalangeal cell and IHC (Fig. 7*A,C*). The P2X$_2$ receptor immunolabeling included the spiral limbus and extended laterally to the spiral ligament, including the Böettcher's cells and root processes of the external sulcus cells. The mesenchymal cells facing scala tympani under the basilar membrane and lining scala vestibuli were devoid of immunostaining.

Both immunoperoxidase and two-photon immunofluorescence imaging showed punctate labeling of the synaptic region below the OHC (Figs. 7*A,C*, 8*A,B*). This labeling was localized to the postsynaptic thickening of type II afferent neuron synapses by immunoelectron microscopy (Fig. 8*C*). The OHC efferent synapses, which are principally cholinergic (Sobkowicz and Emmerling, 1989; Housley and Ashmore, 1991), did not exhibit any P2X$_2$ receptor immunogold labeling (Fig. 8*C*). Extensive punctate P2X$_2$ receptor immunolabeling of the inner radial fiber synaptic processes surrounding the basolateral region of the IHC was clearly apparent at the light microscopic level (Figs. 7*A,C*, 9*B*). Immunogold labeling localized the P2X$_2$ receptor expression to the postsynaptic thickenings of many of these afferent synapses with the IHC (Fig. 9*C,D*), consistent with a purinergic element of
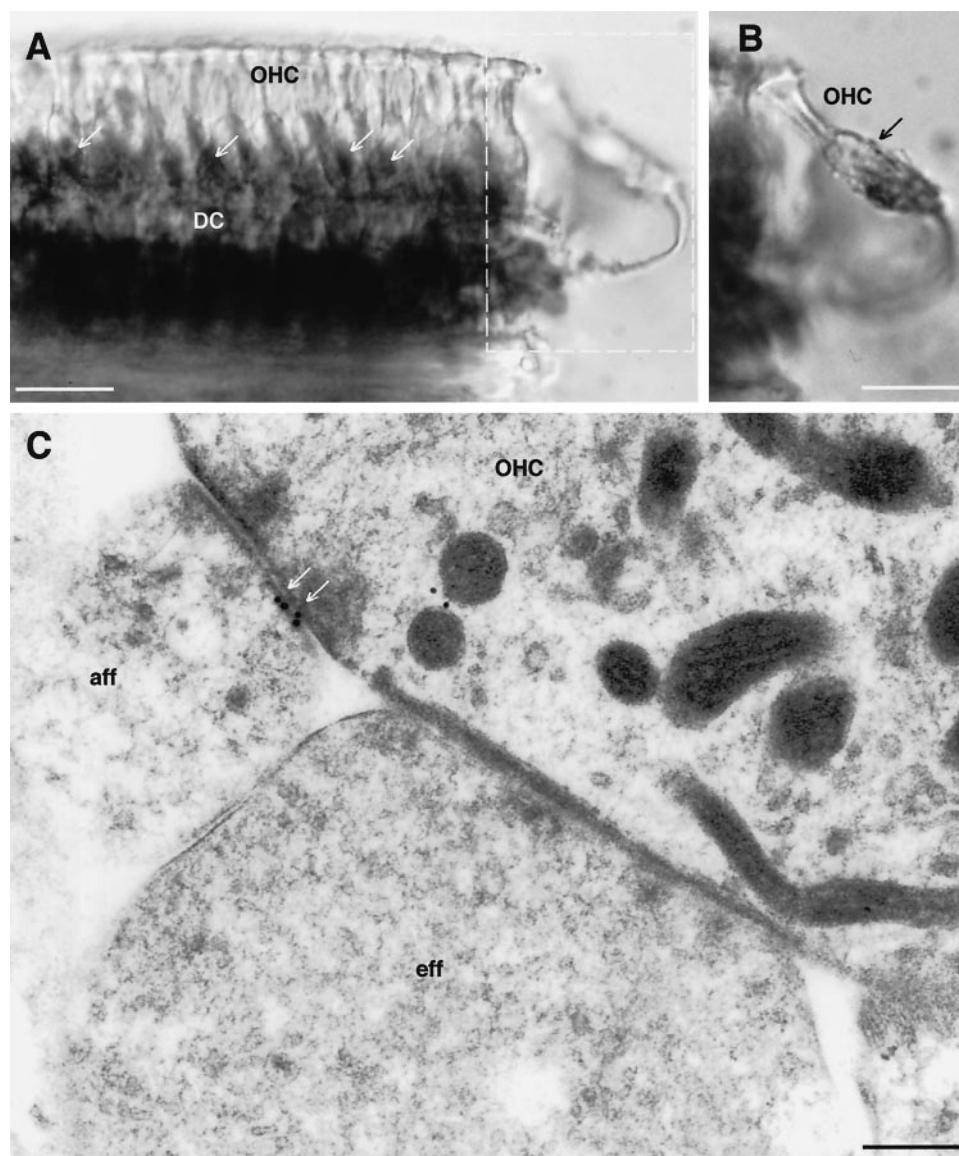
Figure 8. Localization of P2X$_2$ receptor expression associated with the sensory region of the OHC. *A,* Immunoperoxidase labeling of a whole-mount preparation of OHC and associated Deiters' cells (*DC*). Note that, although the body of the OHC is unlabeled, punctate staining is apparent at the base of the OHC (*arrows*) in addition to the more diffuse immunostaining of the Deiters' cells. *B,* Detail of the OHC boxed as out of focus in *A,* which has detached from the body of cells and clearly demonstrates the Deiters' cells cup region supporting the base of the OHC. Punctate synapse-like immunolabeling is associated with this region (*arrow*). *C,* Immunogold labeling of the postsynaptic thickening of the OHC–type II spiral ganglion neuron (afferent) synapse (*aff, arrows*). An adjacent efferent (*eff*) synapse is unlabeled. Scale bars: *A, B,* 20 μm; *C,* 0.2 μm.
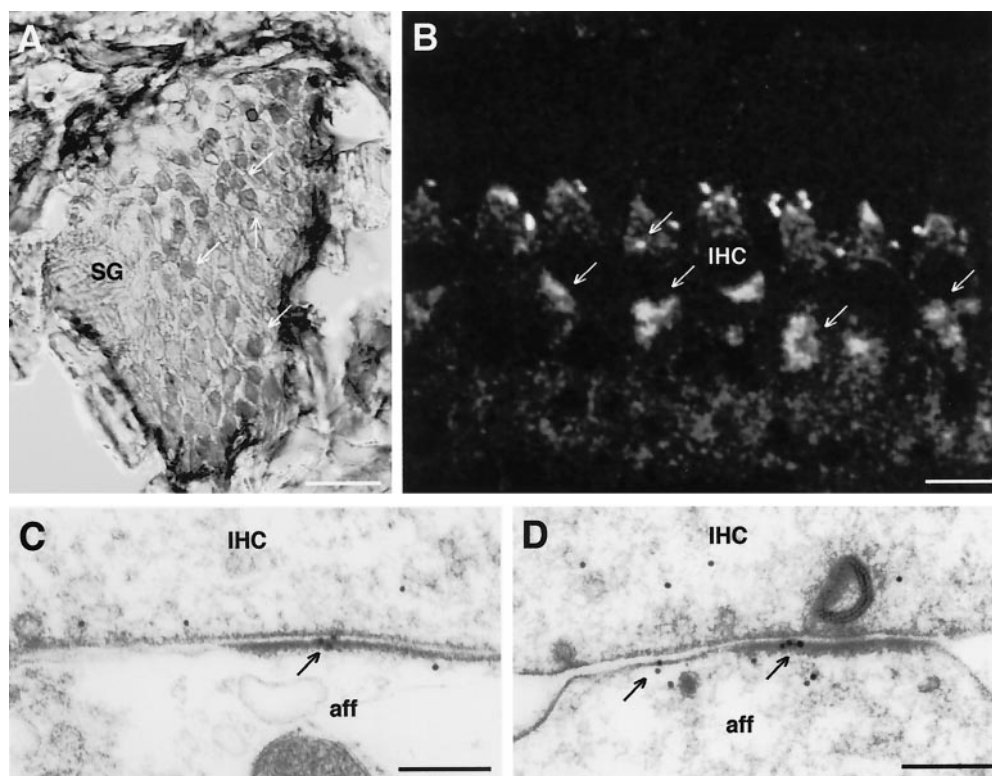
the type I spiral ganglion neuron innervation of these cells. Not all afferent synapses on a given IHC exhibited P2X$_2$ immunogold labeling. Consistent with this finding, sectioned cochlear spiral ganglion showed weak immunopositive labeling of many, but not all, of the spiral ganglion neurons (Fig. 9*A*).

DISCUSSION

Our demonstration of an extensive distribution of P2X$_2$ receptor subunit expression in the guinea pig cochlea provides evidence for divergent roles for extracellular ATP acting via ATP-gated ion channels. The P2X$_2$ receptor expression in cells lining the endolymphatic compartment is compatible with an ATP-activated shunt conductance affecting sound transduction both directly at the stereocilia of the hair cells and via alteration in the electrochemical gradient across the cochlear partition. The expression in the Deiters' cells likely reflects a P2X$_2$ receptor-mediated regulation of micromechanics. Demonstration of these ionotropic receptors at the afferent postsynaptic membranes associated with type I and type II spiral ganglion neuron innervation of IHC and OHC, respectively, provides strong support for a purinergic signaling component in auditory neurotransmission.

Expression of P2X$_{2-1}$ receptor mRNA in organ of Corti is compatible with the nondesensitizing ATP-gated inward current responses and associated P2 receptor pharmacological profile of the guinea pig cochlear hair cells, based on comparison with heterologously expressed P2X$_2$ receptors (Brake et al., 1994; Surprenant et al., 1995; Buell et al., 1996; Evans et al., 1996). In contrast, the guinea pig spiral ganglion neurons express the P2X$_{2-2}$ receptor isoform, which is produced by alternative splicing of exon 11, and demonstrates desensitization with prolonged exposure to ATP (Brändle et al., 1997). We have demonstrated previously by RT-PCR that rat spiral ganglion neurons express P2X$_{2-1}$, P2X$_{2-2}$, and P2X$_{2-3}$ receptor mRNA (Salih et al., 1998). Thus, regulation by alternative splicing appears to be a feature of P2X receptor expression in the cochlea. This is supported by the identification of a number of P2X$_2$ receptor splice variants in a guinea pig organ of Corti cDNA library (Parker et al., 1998). The present study would suggest that the desensitization of the inward current through the ATP-gated ion channels is important at hair cell–afferent neuron synapses but not at the hair cell stereocilia expression site.

Figure 9. Characterization of P2X$_2$ receptor expression associated with the auditory afferent–inner hair cell synapse. *A*, Immunoperoxidase labeling of a subgroup of (principally type I) spiral ganglion neurons (*arrows*) after permeabilization with Triton X-100 (P2X$_2$R96ab 1:4000). *B*, Two-photon P2X$_2$ receptor immunofluorescence optical section showing punctate labeling at the level of the IHC synaptic specialization in the turn two to three region [P2X$_2$R96ab, 1:400; secondary antibody (Alexa 488-conjugated goat antirabbit IgG), 1:400]. *C*, *D*, Immunogold localization of P2X$_2$ receptor subunits on the postsynaptic thickening of type I spiral ganglion neuron–inner hair cell synapses (*arrows*). *A* and *B* were obtained from 20 μm cryosections. Scale bars: *A*, 25 μm; *B*, 10 μm; *C*, *D*, 0.2 μm.

Immunolocalization of P2X$_2$ receptor expression in the cochlea, using an antiserum that does not discriminate between these alternatively spliced isoforms of the P2X$_2$ receptor, provides insight into putative neurohumoral regulatory functions of ATP in the cochlea. The visualization of these ATP-gated ion channel subunits at high density on the hair cell stereocilia resolves a pathway for shunting current in parallel to the transducer current that enters the cells through stretch-gated cation channels (mechanoelectrical transducer or MET channels) also localized at this site (Denk et al., 1995). We have proposed previously a localization of ATP-gated ion channels at the apical surface of the hair cells based on electrophysiological (Housley et al., 1992, 1993; Housley, 1998) and indirect fluorescence imaging (Mockett et al., 1994; Housley et al., 1998a). Outer hair cell ATP-activated conductances increase in a tonotopic manner toward the basal (high frequency) encoding region of the organ of Corti (Raybould and Housley, 1997), varying in number from ~2500 to 8000. In contrast, there are only an estimated 100–150 MET channels per hair cell (Ashmore, 1994; Torre et al., 1995). Given that recent data suggests that each ATP-gated ion channel is assembled as a hexamer of P2X receptor subunits (Nicke et al., 1998), it is likely that between 15,000 and 48,000 P2X$_2$ receptor epitope sites are present principally on the apical-most region of the stereocilia of each hair cell.

The binding of the antiserum-coupled microspheres to the stereocilia of the OHC provides direct proof of the proposed topology of the P2X receptor subunit, which has intracellular N- and C-terminal domains, with the target epitope lying within the putative extracellular domain (Brake et al., 1994). The lack of effect of the P2X$_2$R96ab antiserum on the ATP-gated current is not surprising given recent modeling and experimental data that suggests that the nucleotide binding site and pore-lining region occur just before the M2 domain (Hansen et al., 1997; Rassendren et al., 1997; Newbolt et al., 1998; Torres et al., 1998).

The distribution pattern of P2X$_2$ receptor protein expression in the guinea pig cochlea reported here closely matches the P2X$_2$ receptor mRNA labeling within cell somata described previously for rat and guinea pig cochlear tissue (Housley and Ryan, 1997; Housley et al., 1998b; Parker et al., 1998; Salih et al., 1998). However, the protein labeling demonstrates targeting to specific cellular structures, such as the hair cell stereocilia and the spiral ganglion afferent processes innervating the IHC and OHC. Although the expression of P2X$_2$ receptor subunits by cells lining the endolymphatic compartment is extensive, both *in situ* hybridization studies and our immunocytochemical data indicate that the stria vascularis region is an exception. Interestingly, this site is known to express G-protein-coupled P2Y receptors (metabotropic ATP receptors), which regulate the IsK/KvLQT1 channels responsible for the transport of K$^+$ from the marginal cells into scala media (Marcus et al., 1998).

The present study provides a characterization of the cellular structures in addition to the hair cells and Reissner's membrane, which are involved in the ATP-activated endocochlear shunt (Housley et al., 1997, 1998a,b; Housley, 1998; King et al., 1998). These include the endolymphatic surfaces of the inner and external sulcus cells, as well as elements of the supporting cells of the organ of Corti. Given the apparent low nanomolar levels of endogenous ATP present in endolymph (Muñoz et al., 1995b), it is unlikely that the P2X receptors contribute substantially to the "silent current" (Zidanic and Brownell, 1990). Under stressor conditions, such as noise or ischemia, it is likely that release of ATP into scala media results in substantial activation of the distributed ATP-gated ion channel-mediated shunt conductance out of scala media. ATP is stored in the organ of Corti (Wangemann, 1996) and in the marginal cells of the stria vascularis (White et al., 1995). This shunt has been demonstrated as a fall in cochlear partition resistance (Housley et al., 1997, Thorne et al., 1999) associated with the rapid decline in endocochlear potential,
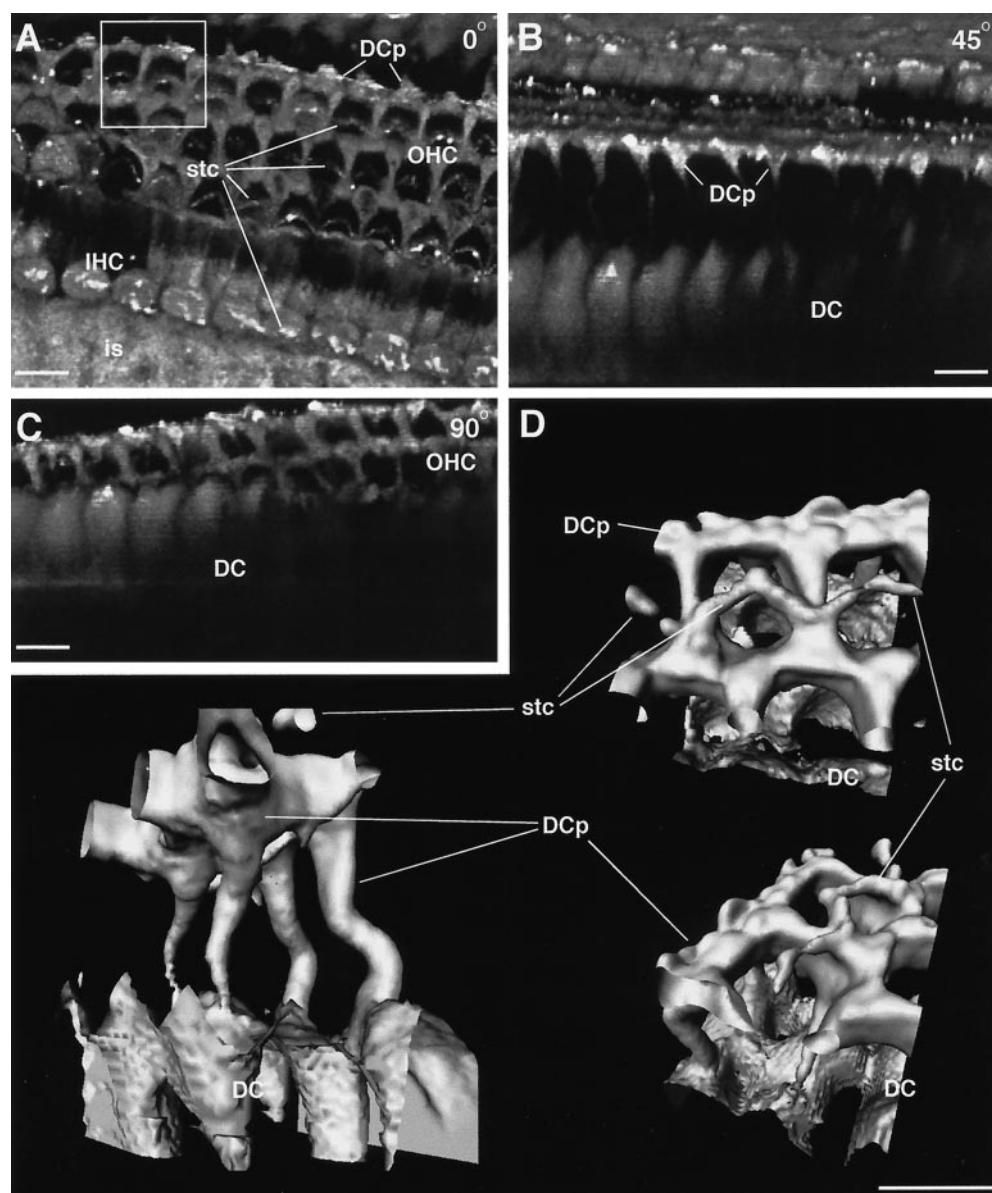
Figure 10. Reconstruction of P2X₂ receptor protein expression in the organ of Corti from confocal immunofluorescence. *A–C* show progressive aspects of a 90 μm^3 of organ of Corti from turn one reconstructed using VoxelView software. The reconstructed image has been rotated relative to the imaging plane, which passed down through the hair cells from their stereocilia (*stc*). *B* and *C* show side views of the Deiters' cells (*DC*), with their processes (*DCp*) extending to support the cuticular plate region of the OHC. Note that, apart from the stereocilia (*stc*) labeling (*A*) and a few OHC cuticular plates, the rest of the OHC membrane is not labeled. The voxel resolution is 0.75 μm^3. Inner sulcus cells, *is*. *D*, Views of an isosurface rendering of P2X₂ receptor protein expression computed from a subset (*box* in *A*) of the serial confocal optical section stack reconstructed in *A–C*. Stereocilia of two OHC are shown by P2X₂ immunofluorescence labeling, although the body of the OHC is unlabeled and therefore not visible. This provides an unparalleled view of the immunolabeling on the associated Deiters' cell processes extending to the reticular lamina and Deiters' cell cup regions, which support the base of the OHC (see Fig. 7*C*, *inset*). Scale bars: *A–C*, 10 μm; *D*, 15 μm.

which occurs when ATP is injected into scala media (Muñoz et al., 1995a; Kirk and Yates, 1998). This pathway is well placed to contribute to altered hearing sensitivity and temporary threshold shift phenomena and to serve a protective role, decoupling the "cochlear amplifier" (Ashmore, 1994) in response to cochlear stressors.

Within the perilymphatic compartment, elevation of extracellular ATP could produce a depolarization and elevation of intracellular Ca^{2+} in the supporting cells in the organ of Corti. In the case of the Deiters' cells, it has been proposed previously that such effects may lead to a change in the micromechanics of these cells, which could affect the coupling of the OHC electromotility to the basilar membrane (Dulon, 1995; Chen and Bobbin, 1998). Our image reconstruction of the extensive expression of P2X₂ receptor subunits over the surface of the Deiters' cells (Fig. 10*D*) suggests a distributed ATP-mediated action across all of the Deiters' cell processes, dependent on ATP levels in the space of Nuel.

There is considerable evidence that P2X₂ receptors are associated with ATP-mediated neurotransmission in the CNS (Simon

et al., 1997; Kanjhan et al., 1999). The detection here of P2X₂₋₂ receptor mRNA expression by spiral ganglion neurons, and particularly our immunogold localization of P2X₂ receptor subunits to the postsynaptic membrane associated with afferent synaptic innervation of IHC and OHC, supports a putative auditory neurotransmitter or neuromodulatory role for ATP.

In the case of the IHC synapse, it is clear that not all type I spiral ganglion neurons expressed the P2X₂ subunit protein, and we found examples of afferent synapses lacking immunogold labeling. This is consistent with the expression of P2X₂ receptor mRNA by ~50% of the spiral ganglion neurons in the rat cochlea (Salih et al., 1998). These data are therefore supportive of a putative submodality of auditory purinergic neurotransmission operating in conjunction with the established glutamatergic neurotransmission (Eybalin, 1993; Matsubara et al., 1996; Niedzielski et al., 1997; Ottersen et al., 1998).

The present data represents the first identification of receptors for a fast neurotransmitter at the type II spiral ganglion afferent fiber–OHC synapse and therefore promotes ATP as a candidate neurotransmitter at this site. In contrast to the IHC–afferent fiber

synapse, GluR expression is notably absent from the afferent synapses with the OHC (Matsubara et al., 1996; Niedzielski et al., 1997). Virtually nothing is known about the physiological role of type II spiral ganglion auditory neurons, which comprise ~5% of the spiral ganglion neuron population and have overlapping central projections with the type I spiral ganglion neurons (Brown, 1988). Previous electrophysiological analysis failed to detect action potentials in a type II spiral ganglion neuron using sound stimuli which drive type I spiral ganglion neurons (Robertson, 1984). In light of the present findings, future studies of afferent transmission may usefully explore more diverse types of OHC stimulation.

In conclusion, this characterization of P2X$_2$ receptor expression provides direct molecular physiological evidence for multiple ATP signaling pathways using P2X$_2$ receptors in the cochlea and provides a platform for addressing unanswered questions on the physiological significance for hearing of P2X receptor expression. These data focus attention on purinergic regulation of sound transduction, modulation of micromechanics of the organ of Corti, and purinergic signaling in auditory afferent neurotransmission.

REFERENCES

Ashmore JF (1994) The G. L. Brown Prize Lecture. The cellular machinery of the cochlea. Exp Physiol 79:113–134.

Bobbin RP, Thompson MH (1978) Effects of putative transmitters on afferent cochlear transmission. Ann Otol Rhino Laryngol 87:185–190.

Brake AJ, Wagenbach MJ, Julius D (1994) New structural motif for ligand-gated ion channels defined by an ionotropic ATP receptor. Nature 371:519–523.

Brändle U, Spielmanns P, Osteroth R, Sim J, Surprenant A, Buell G, Ruppersberg JP, Plinkert PK, Zenner H-P, Glowatzki E (1997) Desensitization of the P2X$_2$ receptor controlled by alternative splicing. FEBS Lett 404:294–298.

Brown MC, Berglund AM, Kiang NY, Ryugo DK (1988) Central trajectories of type II spiral ganglion neurons. J Comp Neurol 287:581–590.

Buell G, Lewis C, Collo G, North RA, Surprenant A (1996) An antagonist-insensitive P2x receptor expressed in epithelia and brain. EMBO J 15:55–62.

Burnstock G (1996) A unifying purinergic hypothesis for the initiation of pain. Lancet 347:1604–1605.

Chen C, Bobbin RP (1998) P2X receptors in cochlear Deiters' cells. Br J Pharmacol 124:337–344.

Chen C, Skellett RA, Fallon M, Bobbin RP (1998) Additional pharmacological evidence that endogenous ATP modulates cochlear mechanics. Hear Res 118:47–61.

Collo G, North RA, Kawashima E, Merlo-Pich E, Neidhart S, Surprenant A, Buell G (1996) Cloning of P2X$_5$ and P2X$_6$ receptors and the distribution and properties of an extended family of ATP-gated ion channels. J Neurosci 16:2495–2507.

Cook SP, Vulchanova L, Hargreaves KM, Elde R, McCleskey EW (1997) Distinct ATP receptors on pain-sensing and stretch-sensing neurons. Nature 387:505–508.

Denk W, Holt JR, Shepherd GMG, Corey DP (1995) Calcium imaging of single stereocilia in hair cells—localization of transduction channels at both ends of tip links. Neuron 15:1311–1321.

Dulon D (1995) Ca^{2+} signalling in Deiters' cells of the guinea-pig cochlea: active process in supporting cells? In: Active hearing (Flock Å, Ottoson D, Ulfendahl M, eds), pp. 195–207. Oxford: Pergamon.

Evans RJ, Lewis C, Virginio C, Lundstrom K, Buell G, Surprenant A, North RA (1996) Ionic permeability of, and divalent cation effects on, two ATP-gated cation channels (P2X receptors) expressed in mammalian cells. J Physiol (Lond) 497.2:413–422.

Eybalin M (1993) Neurotransmitters and neuromodulators of the mammalian cochlea. Physiol Rev 73:309–373.

Glowatzki E, Wild K, Brändle U, Fakler G, Fakler B, Zenner H-P, Ruppersberg JP (1995) Cell-specific expression of the α9-ACh receptor subunit in auditory hair cells revealed by single-cell RT-PCR. Proc R Soc Lond B Biol Sci 262:141–147.

Greenwood D, Yao WP, Housley GD (1997) Expression of the P2X$_2$ receptor subunit of the ATP-gated ion channel in the retina. NeuroReport 8:1083–1088.

Hansen MA, Barden JA, Balcar VJ, Keay KA, Bennett MR (1997) Structural motif and characteristics of the extracellular domain of P2X receptors. Biochem Biophys Res Commun 236:670–675.

Housley GD (1998) Extracellular nucleotide signaling in the inner ear. Mol Neurobiol 16:21–48.

Housley GD (1999) Nucleoside and nucleotide transmission in sensory systems. In: Purinergic and pyrimidinergic signalling, Chap 11, Handbook of experimental pharmacology. Heidelberg: Springer-Verlag.

Housley GD, Ashmore JF (1991) Direct measurement of the action of acetylcholine on isolated outer hair cells of the guinea pig cochlea. Proc R Soc Lond B Biol Sci 244:161–167.

Housley GD, Ryan AF (1997) Cholinergic and purinergic neurohumoral signalling in the inner ear: a molecular physiological analysis. Audiol Neurootol 2:92–110.

Housley GD, Greenwood D, Ashmore JF (1992) Localization of cholinergic and purinergic receptors on outer hair cells isolated from the guinea-pig cochlea. Proc R Soc Lond B Biol Sci 249:265–273.

Housley GD, Greenwood D, Mockett BG, Muñoz DJB, Thorne PR (1993) Differential actions of ATP-activated conductances in outer and inner hair cells isolated from the guinea-pig organ of Corti: a humoral purinergic influence on cochlear function. In: Biophysics of hair cell sensory systems (Duifhuis H, Horst JW, van Dijk P, van Netten SM, eds), pp. 116–123. Singapore: World Scientific.

Housley GD, Greenwood D, Bennett T, Ryan AF (1995) Identification of a short form of the P2xR1-purinoceptor subunit produced by alternative splicing in the pituitary and cochlea. Biochem Biophys Res Commun 212:501–508.

Housley GD, Thorne PR, Kanjhan R, Raybould NP, Muñoz DJB, Luo L, Ryan AF (1997) Regulation of the electrochemical gradient for sound transduction by ATP-gated ion channels on cochlear hair cell stereocilia. Soc Neurosci Abstr 23:731.

Housley GD, Raybould NP, Thorne PR (1998a) Fluorescence imaging of Na$^+$ influx via P2X receptors in cochlear hair cells. Hear Res 119:1–13.

Housley GD, Luo L, Ryan AF (1998b) Localization of mRNA encoding the P2X$_2$ receptor subunit of the adenosine 5′-triphosphate-gated ion channel in the adult and developing rat inner ear by in situ hybridization. J Comp Neurol 393:403–414.

Kanjhan R, Housley GD, Thorne PR, Christie DL, Palmer DJ, Luo L, Ryan AF (1996) Localization of ATP-gated ion channels in cerebellum using P2x$_2$R subunit-specific antisera. NeuroReport 7:2665–2669.

Kanjhan R, Housley GD, Burton LD, Christie DL, Kippenberger A, Thorne PR, Luo L, Ryan AF (1999) Distribution of the P2X$_2$ receptor subunit of the ATP-gated ion channels in the rat central nervous system. J Comp Neurol 407:11–32.

King M, Housley GD, Raybould NP, Greenwood D, Salih SG (1998) Expression of ATP-gated ion channels by Reissner's membrane epithelial cells. NeuroReport 9:2467–2474.

Kirk DL, Yates GK (1998) ATP in endolymph enhances electrically-evoked oto-acoustic emissions from the guinea pig cochlea. Neurosci Lett 250:149–152.

Kujawa SG, Erostegui C, Fallon M, Crist J, Bobbin RP (1994) Effects of adenosine 5′-triphosphate and related agonists on cochlear function. Hear Res 76:87–100.

Marcus DC, Sunose H, Liu JZ, Bennett T, Shen ZJ, Scofield MA, Ryan AF (1998) Protein kinase C mediates P-2u purinergic receptor inhibition of K$^+$ channel in apical membrane of strial marginal cells. Hear Res 115:82–92.

Matsubara A, Laake JH, Davanger S, Usami S, Ottersen OP (1996) Organization of AMPA receptor subunits at a glutamate synapse: a quantitative immunogold analysis of hair cell synapses in the rat organ of Corti. J Neurosci 16:4457–4467.

Mockett BG, Housley GD, Thorne PR (1994) Fluorescence imaging of extracellular purinergic receptor sites and putative ecto-ATPase sites on isolated cochlear hair cells. J Neurosci 14:6992–7007.

Muñoz D, Thorne P, Housley G, Billett T, Battersby J (1995a) Extracellular adenosine 5′-triphosphate (ATP) in the endolymphatic compartment influences cochlear function. Hear Res 90:106–118.

Muñoz D, Thorne P, Housley G, Billett T (1995b) Adenosine 5′-triphosphate (ATP) concentrations in the endolymph and perilymph of the guinea-pig cochlea. Hear Res 90:119–125.

Newbolt A, Stoop R, Virginio C, Surprenant A, North RA, Buell G,

Rassendren F (1998) Membrane topology of an ATP-gated ion channel (P2X receptor). J Biol Chem 273:15177–15182.

Nicke A, Baumert HG, Rettinger J, Eichele A, Lambrecht G, Mutschler E, Schmalzing G (1998) P2X1 and P2X3 receptors form stable trimers: a novel structural motif of ligand-gated ion channels. EMBO J 17:3016–3028.

Niedzielski AS, Safieddine S, Wenthold RJ (1997) Molecular analysis of excitatory amino acid receptor expression in the cochlea. Audiol Neurootol 2:79–91.

North RA (1996) Families of ion channels with two hydrophobic segments. Curr Opin Cell Biol 8:474–483.

Ottersen OP, Takumi Y, Matsubara A, Landsend AS, Laake JH, Usami S (1998) Molecular organization of a type of peripheral glutamate synapse: the afferent synapses of hair cells in the inner ear. Prog Neurobiol 54:127–148.

Parker MS, Larroque ML, Campbell JM, Bobbin RP, Deininger PL (1998) Novel variant of the P2X$_2$ ATP receptor from the guinea pig organ of Corti. Hear Res 121:62–70.

Rassendren F, Buell G, Newbolt A, North RA, Surprenant A (1997) Identification of amino acid residues contributing to the pore of a P2X receptor. EMBO J 16:3446–3454.

Raybould NP, Housley GD (1997) Variation in expression of the outer hair cell P2X receptor conductance along the guinea-pig cochlea. J Physiol (Lond) 498.3:717–727.

Robertson D (1984) Horseradish peroxidase injection of physiologically characterized afferent and efferent neurones in the guinea pig spiral ganglion. Hear Res 15:113–121.

Salih SG, Housley GD, Burton LD, Greenwood D (1998) P2X$_2$ receptor subunit expression in a subpopulation of cochlear type I spiral ganglion neurones. NeuroReport 9:279–282.

Simon J, Kidd EJ, Smith FM, Chessell IP, Murrell-Lagnado R, Humphrey PPA, Barnard EA (1997) Localization and functional expression of splice variants of the P2X$_2$ receptor. Mol Pharmacol 52:237–248.

Sobkowicz HM, Emmerling MR (1989) Development of acetylcholinesterase-positive neuronal pathways in the cochlea of the mouse. J Neurocytol 18:209–224.

Soeller C, Cannell MB (1996) Construction of a two-photon microscope and optimisation of illumination pulse duration. Pflügers Arch 432:555–561.

Sugasawa M, Erostegui C, Blanchet C, Dulon D (1996) ATP activates a cation conductance and a Ca^{2+}-dependent Cl$^-$ conductance in Hensen's cells of the guinea-pig cochlea. Am J Physiol 271:C1817–C1827.

Surprenant A, Buell G, North RA (1995) P2X receptors bring new structure to ligand-gated ion channels. Trends Neurosci 18:224–229.

Thorne PR, Housley GD (1996) Purinergic signalling in sensory systems. Semin Neurosci 8:233–246.

Thorne PR, Muñoz DJB, Housley GD, Vlajkovic S, Kendrick IS, Rasam M (1999) Regulation of cochlear sensitivity by extracellular ATP. Proceedings of the 22nd Annual midwinter meeting, Association of Research in Otolaryngology, St. Petersburg, FL.

Torre V, Ashmore JF, Lamb TD, Menini A (1995) Transduction and adaptation in sensory receptor cells. J Neurosci 15:7757–7768.

Torres GE, Egan TM, Voigt MM (1998) Topological analysis of the ATP-gated ionotropic P2X$_2$ receptor subunit. FEBS Lett 425:19–23.

Usami S, Osen KK, Zhang N, Ottersen OP (1992) Distribution of glutamate-like and glutamine-like immunoreactivities in the rat organ of Corti: a light microscopic and semiquantitative electron microscopic analysis with a note on the localization of aspartate. Exp Brain Res 91:1–11.

Vlajkovic S, Thorne PR, Housley GD, Muñoz DJB, Kendrick IS (1998a) Ecto-nucleotidases terminate purinergic signalling in the cochlear endolymphatic compartment. NeuroReport 9:1559–1565.

Vlajkovic S, Thorne PR, Housley GD, Muñoz DJB, Kendrick IS (1998b) The pharmacology and kinetics of ecto-nucleotidases in the perilymphatic compartment of the guinea-pig cochlea. Hear Res 117:71–80.

Wangemann P (1996) Ca^{2+}-dependent release of ATP from the organ of Corti measured with a luciferin-luciferase bioluminescence assay. Audit Neurosci 2:187–192.

White P, Thorne P, Housley G, Mockett B, Billett T, Burnstock G (1995) Quinacrine staining of marginal cells in the stria vascularis of the guinea-pig cochlea: a possible source of extracellular ATP? Hear Res 90:97–105.

Zidanic M, Brownell WE (1990) Fine structure of the intracochlear potential field. I. The silent current. Biophys J 57:1253–1268.